Two spheres in a free stream of a second-order fluid

A. M. Ardekani[1], R. H. Rangel[1], and D. D. Joseph[1,2]

[1]*Department of Mechanical and Aerospace Engineering*

University of California, Irvine, CA 92697 and

[2]*Department of Aerospace Engineering and Mechanics*

University of Minnesota, MN 55455

7 March 2008

Abstract

The forces acting on two fixed spheres in a second-order uniform flow are investigated. When $\alpha_1 + \alpha_2 = 0$, where α_1 and α_2 are fluid parameters related to the first and second normal stress coefficients, the velocity field for a second-order fluid is the same as the one predicted by the Stokes equations while the pressure is modified. The Stokes solutions given by Stimson and Jeffery [Proc. R. Soc. London, Ser. A 111, 110 (1926)] for the case when the flow direction is along the line of centers and Goldman *et al.*[Chemical Eng. Science 21, 1151 (1966)] for the case when the flow direction is perpendicular to the line of centers are utilized and the stresses and the forces acting on the particles in a second-order fluid are calculated. For flow along the line of centers or perpendicular to it, the net force is in the direction that tends to decrease the particle separation distance. For the case of flow at arbitrary angle, unequal forces are applied to the spheres perpendicularly to the line of centers. These forces result in a change of orientation of the sedimenting spheres until the line of centers aligns with the flow direction. In addition, the potential flow of a second-order fluid past two fixed spheres in uniform flow is investigated. The normal stress at the surface of each sphere is calculated and the viscoelastic effects on the normal stress for different separation distances are analyzed. The contribution of the potential flow of a second-order fluid to the force applied to the particles is an attractive force. Our explanations of the aggregation of particles in viscoelastic fluids rest on three pillars; the first is a viscoelastic "pressure" generated by normal stresses due to shear. Secondly, the total time derivative of the pressure is an important factor in the forces applied to moving particles. The third is associated with a change in the normal stress at points of stagnation which is a purely extensional effect unrelated to shearing.

1. INTRODUCTION

The motion of small particles at low Reynolds number was comprehensively reviewed by Happel and Brenner[1] and by Goldsmith and Mason[2]. Extensive reviews on the motion of particles in non-Newtonian fluids were reported by Caswell[3] and Leal[4]. More recently, the unsteady motion of solid spheres and their collisions have been studied by Ardekani and Rangel[5,6]. In this study, the forces acting on two spherical particles in a second-order fluid are investigated.

If two spheres are set into motion in a viscoelastic fluid in an initial side-by-side configuration in which the two spheres are separated by a smaller than critical gap, the spheres will attract, turn and chain[7]. In the sedimentation of a transversely isotropic particle at low Reynolds number through a quiescent fluid, the presence of even weak viscoelasticity is responsible for adaption of a specific orientation independent of the initial configuration, whereas in a Newtonian fluid, the particle configuration is indeterminant at zero Reynolds number[4]. Similarly, two spherical particles sediment in a Newtonian fluid with constant orientation equal to their initial orientation, whereas particles tend to line up in a viscoelastic fluid. Our interest is to see if a second-order fluid model can predict the orientation of two sedimenting particles.

Expansion of the general stress function for slow and slowly varying motion gives rise to the second-order fluid introduced by Coleman and Noll[8–11]. Correct predictions have been obtained for second-order fluids for the orientation of a settling long body, the evolution of the Jeffery orbit[12] and the lateral migration of a sphere in a non-homogeneous shear flow[13]. However, the predictions of the fluid response to rapid motions have not been satisfactory.

The motion of a spherical particle normal to a wall in a second-order fluid was investigated theoretically by Ardekani *et al.*[14] who showed that the contribution of the second-order fluid to the overall force applied to the particle is an attractive force towards the wall independent of the direction of motion of the particle.

Riddle *et al.*[15] experimentally studied the effect of the distance between two identical spheres falling along their line of centers in viscoelastic fluids and found that the gradual separation or coalescence of two spheres depends on their initial separation distance. Brunn[16] considered the interaction of two identical spheres sedimenting in a quiescent second-order fluid and observed that the distance between spheres decreases as they fall. His analysis

applies when the particle separation is large and he did not find a critical separation distance for attraction. Brunn[17] analyzed sedimentation of particles of arbitrary shape in a second-order fluid. His investigation shows that a transversely isotropic particle changes orientation until it becomes either parallel or perpendicular to the direction of the external force.

Phillips[18] developed a method to calculate the motion of N spherical particles suspended in a quiescent second-order fluid in a low-Reynolds-number flow. Binous and Phillips[19] used a modified version of the Stokesian dynamics method to calculate directly the particle-particle and particle-bead interactions. In their approach, a viscoelastic fluid is represented as a suspension of finite-extension, non-linear, elastic dumbbells in a Newtonian solvent. They showed that two sedimenting spheres are in most cases attracted to each other and turn in such way that their line-of-centers is in the direction of gravity. Bot *et al.*[20] experimentally investigated the motion of two identical spheres along the center line of a cylindrical tube filled with a Boger fluid. They observed that the spheres attract for large distances but separate for small distances. Feng *et al.*[21] presented a two-dimensional numerical study of particle-particle and particle-wall interactions in an Oldroyd-B fluid and they observed that two particles settling side by side attract and approach each other. The doublet rotates until the line of centers is aligned with the direction of fall. More recently, Phillips and Talini[22] studied hydrodynamic interactions between widely separated spheres utilizing a multipole expansion and observed particles chaining in sedimentation and shear flows.

In the present study, two non-rotating and freely rotating, fixed spheres in a uniform flow of a second-order fluid at an arbitrary direction using Stokes equations are discussed. The results utilizing Stokes equations confirm that a viscoelastic pressure associated with high-shear rates on the surface of particles promotes the attraction and alignment of particles in the direction of sedimentation for any range of particles separation. For freely rotating spheres, the time derivative of the Stokes pressure is non zero and it enhances the attraction of the spheres. An important question is whether other mechanisms of attraction or repulsion exist for particles in a second-order fluid. In order to answer this question, we examine the normal stresses at the stagnation points as calculated from viscoelastic potential flow. The literature shows that the sedimenting particles chain robustly in all flows: sedimentation, fluidization, shear flows, oscillating shear flows, and elongational flows. This chaining occurs for particles ranging in sizes from microns to centimeters[7,22]. Therefore, the cause must be local and we believe the local mechanism is due to the change in the normal stress which

we compute in the second-order order fluid. Locally, near the stagnation point, the flow is slow and it could be argued that for this reason the local behavior is second order. Takagi *et al.*[23] similarly use the idea of a local Stokes flow at the boundary of a moving particle. In addition, at the stagnation point, the no-slip condition is satisfied exactly while the slip velocity is small in the vicinity of the stagnation point. This argument supports the idea of examining the normal stresses in the neighborhood of the stagnation point in a second-order fluid using viscoelastic potential flow.

As Harlen *et al.*[24] noted polymers are fully extended in the wake and this generates some problems in numerical simulations of flow around the sphere and the mathematical tools might not be able to predict this full extension of polymeric chains. One might get a large disagreement between the mathematical and experimental results at this region. However, this does not impose any mathematical constraint on the use of the second-order model when $\alpha_1 + \alpha_2 = 0$. Tanner[25] calculated the normal stress difference for steady elongational flow $\mathbf{V} = \dot{\varepsilon}(x\mathbf{i} - \frac{1}{2}y\mathbf{j} - \frac{1}{2}z\mathbf{k})$ using a second-order fluid, where $\mathbf{V}$ is the velocity field, is the strain rate, $\mathbf{i}$, $\mathbf{j}$, $\mathbf{k}$ are unit vectors along x, y, z directions. He found that $\sigma_{xx} - \sigma_{yy} = 3\dot{\varepsilon}\mu_f(1 + \dot{\varepsilon}(\alpha_1 + \alpha_2)/\mu_f)$ leads to unacceptable results at some negative $\dot{\varepsilon}$ with large absolute value since the stress difference and the strain rate have different sign. In this equation, σ and μ_f and represent the stress tensor and fluid viscosity, respectively. This does not occur for the case in which we used the Stokes analysis since $(\alpha_1 + \alpha_2)$. However, for the viscoelastic potential flow analysis, we should consider small values of the Deborah number to avoid this problem.

The governing equations are presented in Section 2. The forces acting on two non-rotating fixed spheres in a uniform flow with arbitrary direction are discussed in Section 3. The forces acting on freely rotating spheres in a free stream are considered in Section 4. It is known that two torque-free spheres falling side by side in Newtonian fluid at low Reynolds number rotate. Thus, in order to fully understand the behavior of falling spheres in a viscoelastic fluid, the forces acting on rotating fixed spheres are calculated. The viscoelastic potential analysis for these two particles in uniform flow along their line of center is presented in section 5.

2. THEORETICAL DEVELOPMENT

The governing equations for a second-order fluid are as follows:

$$\rho_f[\frac{\partial \mathbf{u}}{\partial t} + (\mathbf{u} \cdot \nabla)\mathbf{u}] = \nabla \cdot \mathbf{T} \tag{1}$$

$$\nabla \cdot \mathbf{u} = 0 \tag{2}$$

where $\mathbf{u}$ is the velocity field and ρ_f is the fluid density. The stress tensor $\mathbf{T}$ for an incompressible second-order fluid is

$$\mathbf{T} = -p\mathbf{I} + \mu_f \mathbf{A} + \alpha_1 \mathbf{B} + \alpha_2 \mathbf{A}^2 \tag{3}$$

where p is the pressure, μ_f is the zero shear viscosity, $\mathbf{A} = \nabla \mathbf{u} + \nabla \mathbf{u}^T$ is the symmetric part of velocity gradient and $\mathbf{B}$ is given as

$$\mathbf{B} = \frac{\partial \mathbf{A}}{\partial t} + (\mathbf{u} \cdot \nabla)\mathbf{A} + \mathbf{A}\nabla \mathbf{u} + \nabla \mathbf{u}^T \mathbf{A} \tag{4}$$

with $\alpha_1 = -\frac{\psi_1}{2}$ and $\alpha_2 = \psi_1 + \psi_2$ where ψ_1 and ψ_2 are the first and second normal stress coefficients. In two dimensions or when $\alpha_1 + \alpha_2 = 0$, the velocity field for a second-order fluid is the same as the one predicted by the Stokes flow while the pressure is modified as[25]

$$p = p_N + \frac{\alpha_1}{\mu_f}\frac{Dp_N}{Dt} + \frac{\beta}{4} tr\mathbf{A}^2 \tag{5}$$

where p_N is the Stokes pressure and $\beta = 3\alpha_1 + 2\alpha_2$ is the climbing constant. We shall call $\frac{\beta}{4} tr\mathbf{A}^2$ a viscoelastic "pressure"; it is like a pressure because it is always compressive. The viscoelastic pressure is large when $tr\mathbf{A}^2$ is large and it is large at points on the body where the flow is fastest; just the opposite of inertia. $\frac{\alpha_1}{\mu_f}\frac{Dp_N}{Dt}$ is zero for non-rotating spheres and is non-zero for rotating spheres. For unsteady problems, it could generate a tensile or compressive normal stress. The effect of this term on the forces applied on a sphere moving normal to a wall in a second-order fluid is discussed by Ardekani *et al.*[14]. For a particle nearly touching the wall, $\frac{\alpha_1}{\mu_f}\frac{Dp_N}{Dt}$ is much larger than $\frac{\beta}{4} tr\mathbf{A}^2$ and this results in a large deviation from the Newtonian case and yields a tensile stress at the stagnation point close to the wall.

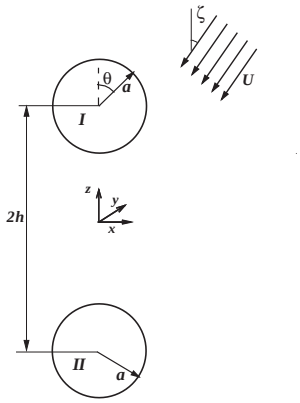

FIG. 1: Two spherical particles in a arbitrary-direction free stream

3. FORCES ACTING ON TWO NON-ROTATING FIXED SPHERES IN A SECOND-ORDER FLUID

The shear and normal stresses applied to two non-rotating fixed particles in a second-order fluid in a uniform free stream are calculated. The schematic of the problem is shown in figure 1. Since the problem is steady and the particles are fixed, a few simplifications can be made and the stress tensor can be written as

$$\mathbf{T}|_{\text{on particle}} = -\left(P_N + \frac{\beta}{4}\mathbf{A} : \mathbf{A}\right)\mathbf{I} + \mu_f \mathbf{A} + \alpha_1 \mathbf{A}\nabla\mathbf{u} + \alpha_1 \nabla\mathbf{u}^T\mathbf{A} + \alpha_2 \mathbf{A}^2 \tag{6}$$

The boundary conditions on the surface of the spheres are more easily expressed in terms of bispherical coordinates. Cylindrical coordinates (r, z, φ) can be transformed to bispherical coordinates (ξ, η, φ) as

$$r = c\frac{\sin\eta}{\cosh\xi - \cos\eta} \qquad z = c\frac{\sinh\xi}{\cosh\xi - \cos\eta} \tag{7}$$

The coordinates (ξ, η, φ) vary in the interval $[-\alpha, \alpha]$, $[0, \pi]$, $[0, 2\pi]$, respectively, where the surface of the spheres are at $\xi = \pm\alpha$ and α and c can be calculated by using the following equations

$$\cosh\alpha = \frac{h}{a} \qquad c = a\sinh\alpha \tag{8}$$

Let $\mu = \cos\eta$. Then $\nabla\mathbf{u}$ in bispherical coordinates can be written as

$$\nabla\mathbf{u}|_{\text{on particle}} = \frac{\cosh\xi - \mu}{c} \times$$
$$\begin{pmatrix} \frac{\partial u_\xi}{\partial\xi} - u_\eta\frac{\sin\eta}{\cosh\xi-\mu} & \frac{\partial u_\xi}{\partial\eta} + u_\eta\frac{\sinh\xi}{\cosh\xi-\mu} & \frac{1}{\sin\eta}\frac{\partial u_\xi}{\partial\varphi} + \frac{u_\phi\sin\eta\sinh\xi}{\sin\eta(\cosh\xi-\mu)} \\ \frac{\partial u_\eta}{\partial\xi} + u_\xi\frac{\sin\eta}{\cosh\xi-\mu} & \frac{\partial u_\eta}{\partial\eta} - u_\xi\frac{\sinh\xi}{\cosh\xi-\mu} & \frac{1}{\sin\eta}\frac{\partial u_\eta}{\partial\varphi} - \frac{u_\phi(\mu\cosh\xi-1)}{\sin\eta(\cosh\xi-\mu)} \\ \frac{\partial u_\varphi}{\partial\xi} & \frac{\partial u_\varphi}{\partial\eta} & \frac{1}{\sin\eta}\frac{\partial u_\varphi}{\partial\varphi} + \frac{-u_\xi\sin\eta\sinh\xi+u_\eta(\mu\cosh\xi-1)}{\sin\eta(\cosh\xi-\mu)} \end{pmatrix} \tag{9}$$

A. Free stream along the line of centers

Stimson and Jeffery[26] solved the axisymmetric problem where two spheres translate along their line of centers using bispherical coordinates. Here we only summarize the results.

The stream function for two translating particles in a quiescent unbounded flow can be written as

$$\psi = (\cosh\xi - \mu)^{-\frac{3}{2}} \sum_{n=1}^{\infty} UX_n \left(P_{n-1}(\mu) - P_{n+1}(\mu)\right) \tag{10}$$

where U is the particle velocity, $P_n(\mu)$ is the Legendre polynomial of degree n and its derivatives can be written as

$$\frac{d^m}{d\mu^m}P_n(\mu) = \frac{(-1)^m}{\sqrt{1-\mu^2}^m}P_n^m(\mu) \tag{11}$$

$$\begin{aligned} X_n &= \hat{A}_n\cosh(n-\frac{1}{2})\xi + \hat{B}_n\sinh(n-\frac{1}{2})\xi \\ &+ \hat{C}_n\cosh(n+\frac{3}{2})\xi + \hat{D}_n\sinh(n+\frac{3}{2})\xi \end{aligned} \tag{12}$$

The coefficients $\hat{A}_n$ through $\hat{D}_n$ are described by Stimson and Jeffery[26]. From the continuity equation in bispherical coordinates and also using a Galilian transformation since we are

interested in the problem of two fixed spheres in a free stream, we can write

$$u_\xi = U\frac{\cosh\xi\mu - 1}{\cosh\xi - \mu} - \frac{(\cosh\xi - \mu)^2}{c^2}\frac{\partial\psi}{\partial\mu}$$
$$u_\eta = U\frac{\sinh\xi\sin\eta}{\cosh\xi - \mu} - \frac{(\cosh\xi - \mu)^2}{c^2\sin\eta}\frac{\partial\psi}{\partial\xi} \tag{13}$$

The pressure P_N can be expressed as an infinite summation of spherical harmonics as follows[27,28]

$$p_N = \frac{1}{c^3}(\cosh\xi - \mu)^{\frac{1}{2}}\sum_{n=0}^{\infty}[A_n\cosh(n+\frac{1}{2})\xi + B_n\sinh(n+\frac{1}{2})\xi]P_n(\mu) \tag{14}$$

The coefficients A_n and B_n are defined by Pasol *et al.*[27]. Calculating u_ξ, u_η, and P_N and using equations (6) and (9) gives the stress tensor T_b in bispherical coordinates. Using the rotation matrix from cylindrical to bispherical coordinates we have

$$R_1 = \begin{pmatrix} \frac{\cosh\xi-\mu}{c}\frac{\partial r}{\partial\xi} & \frac{\cosh\xi-\mu}{c}\frac{\partial z}{\partial\xi} & 0 \\ \frac{\cosh\xi-\mu}{c}\frac{\partial r}{\partial\eta} & \frac{\cosh\xi-\mu}{c}\frac{\partial z}{\partial\eta} & 0 \\ 0 & 0 & 1 \end{pmatrix}, \qquad T_{cyl} = R_1^T T_b R_1 \tag{15}$$

To calculate the stress tensor in spherical coordinates centered at the sphere center (ρ, θ, φ), we have

$$R_2 = \begin{pmatrix} \sin\theta & \cos\theta & 0 \\ \cos\theta & -\sin\theta & 0 \\ 0 & 0 & 1 \end{pmatrix}, \qquad T_{sph} = R_2^T T_{cyl} R_2 \tag{16}$$

Finally, the force applied to each particle can be written as

$$F = 2\pi a^2\int_0^\pi (T_{\rho\rho}\cos\theta - T_{\rho\theta}\sin\theta)\sin\theta d\theta \tag{17}$$

with λ defined as

$$\lambda = \frac{F}{6\pi\mu_f aU} = \lambda_N + \lambda_{De}De \tag{18}$$

where $De = \frac{|\alpha_1|U}{\mu a}$ is the Deborah number. Examining the normal stress in equation (6), the first and third terms result in a force which is the same as the one in a Newtonian liquid. The remaining terms result in a force which is only present in a second-order fluid and is proportional to De. Thus λ, the force on the particle normalized with the Stokes Law drag, is divided into Newtonian and non-Newtonian terms. A schematic of the forces acting on the particles is shown in figure 2 (forces are not to scale). As it can be seen, the contribution of a second-order fluid to the force applied to the particles is attractive. This is in agreement with experimental results by Riddle *et al.*[15] and analytical ones by Brunn[16]. Riddle *et al.*[15] found that the distance between two identical spheres falling along their line of centers gradually increases if their separation is larger than a critical value and decreases otherwise. Brunn[16] analysis applies when the particle separation is large and he did not find a critical separation distance for attraction. Our analysis is valid when the particle separation distance is small and it does not predict any critical separation distance. The normalized force applied to each particle in a Newtonian and a second-order fluid is shown in figure 3(a). This force varies linearly with De. The nondimensional coefficient λ_{De} is shown in figure 3(b). As it can be seen, this attractive force decreases as the separation distance between the particles increases. The present results are quantitatively compared by the results with Brunn[16] in figure 3(b). For large separation between particles, the solutions are the same. However, for small separation distances, Brunn's results overpredict the attraction between particles. The normal and shear stresses and the pressure on the surface of sphere I is shown in figure 4. Superscript * refers to dimensionless parameters. The stresses and pressure are non-dimensionalized by $\frac{1}{2}\rho U^2$. The shear stress is the same for the Newtonian and the second-order fluid. The normal stress and the pressure are also the same for both fluids at the leading ($\theta = 0$) and trailing ($\theta = \pi$) edges. However, they differ noticeably at other angles. A large compressive stress is observed at the side of the sphere for the second-order fluid. The increase in intensity of the compressive normal stresses due to larger shear rate means that the turning couples which rotate long bodies into the stream and the attractive stresses which cause spherical particles to aggregate are all increased.

These calculations can be used for sedimenting particles when the particles reach their terminal velocity and their approaching velocity is small compared to their terminal velocity.

The present results are valid for a fluid in which the second normal stress coefficient is equal to the negative one half of the first normal stress coefficient. However, $\alpha_1 + \alpha_2$ is

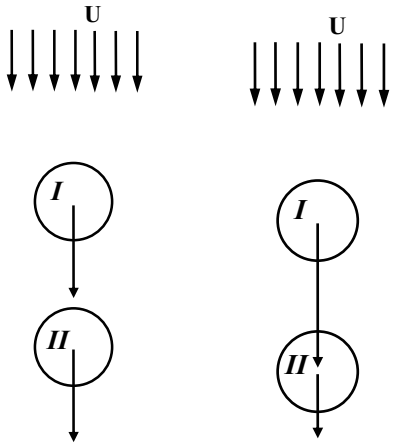

(a) (b)

FIG. 2: Schematic of forces acting on two particles. (a) Newtonian fluid. (b) 2^{nd}-order fluid.

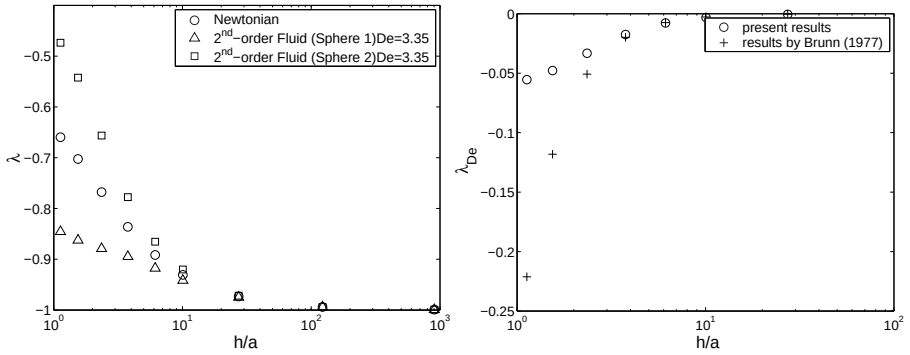

(a) (b)

FIG. 3: Forces acting on particles in a second-order fluid while the free stream is along the particles line of centers.

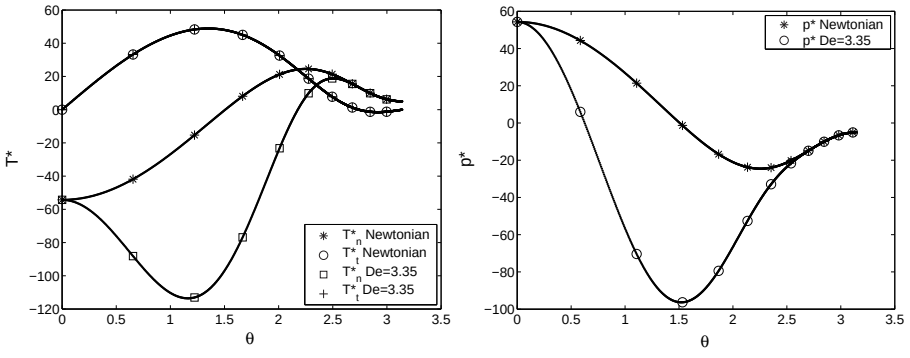

(a) Normal and shear stresses (b) Pressure

FIG. 4: Stresses on the surface of particle I in a second-order fluid while the free stream is along the particles line of centers. $Re = 0.05$, $De = 3.35$, $\frac{h}{a} = 1.543$.

positive for the fluids known to us and for simplification this constraint is applied to the fluid in this section. However, a different method is utilized in the section 5 and the constraint on normal stress coefficients is removed. Ardekani *et al.*[14] utilized a perturbation method for a spherical particle moving normal to a wall when $\epsilon = \frac{h}{a} - 1$ and $\frac{De}{\epsilon}$ are small and there is no constraint on α_1 and α_2. They concluded that the difference between the forces acting on the sphere in second-order and Newtonian fluids is more pronounced as $|\frac{\alpha_2}{\alpha_1}|$ is increased and the force applied to the particle can be written as follows

$$F = -\frac{6\pi\mu_f U a}{\epsilon}\big[1 + \frac{De}{10\epsilon}(2 - 3\frac{\alpha_2}{\alpha_1})\big] \tag{19}$$

The same calculation can be used for this problem when the particles are close to each other.

B. Free stream perpendicular to the line of centers

The motion of two spherical particles perpendicularly to their line of centers has been studied by several investigators[29,30]. Here, the results by Goldman *et al.*[29] are utilized and briefly summarized. The pressure and velocity components can be described as follows

$$p_N^\dagger = \mu_f \frac{U}{c} W^\dagger \cos\varphi \tag{20}$$

$$u_r^\dagger = U\left(-1 + \frac{1}{2c}[rW^\dagger + c(X^\dagger + Y^\dagger)]\right)\cos\varphi = \tilde{u}_r^\dagger \cos\varphi \tag{21}$$

$$u_\varphi^\dagger = U\left(1 + \frac{1}{2}[(X^\dagger - Y^\dagger)]\right)\sin\varphi = \tilde{u}_\varphi^\dagger \sin\varphi \tag{22}$$

$$u_z^\dagger = \frac{1}{2c} U(zW^\dagger + 2cZ^\dagger)\cos\varphi = \tilde{u}_z^\dagger \cos\varphi \tag{23}$$

where the auxiliary functions $W^{\dagger}$, $X^{\dagger}$, $Y^{\dagger}$, and $Z^{\dagger}$ can be written as

$$Z^{\dagger} = (\cosh\xi - \mu)^{\frac{1}{2}} \sin\eta \sum_{n=1}^{\infty} [A_n^{\dagger} \sinh(n+\frac{1}{2})\xi] P_n'(\mu) \tag{24}$$

$$W^{\dagger} = (\cosh\xi - \mu)^{\frac{1}{2}} \sin\eta \sum_{n=1}^{\infty} [B_n^{\dagger} \cosh(n+\frac{1}{2})\xi + C_n^{\dagger} \sinh(n+\frac{1}{2})\xi] P_n'(\mu) \tag{25}$$

$$Y^{\dagger} = (\cosh\xi - \mu)^{\frac{1}{2}} \sum_{n=1}^{\infty} [D_n^{\dagger} \cosh(n+\frac{1}{2})\xi + E_n^{\dagger} \sinh(n+\frac{1}{2})\xi] P_n(\mu) \tag{26}$$

$$X^{\dagger} = (\cosh\xi - \mu)^{\frac{1}{2}} \sin^2\eta \sum_{n=1}^{\infty} [F_n^{\dagger} \sinh(n+\frac{1}{2})\xi + G_n^{\dagger} \sinh(n+\frac{1}{2})\xi] P_n''(\mu) \tag{27}$$

where the coefficients $A_n^{\dagger}$ through $G_n^{\dagger}$ are given by Goldman *et al.*[29] and Goldman[31]. Calculating the velocity field, $\nabla\mathbf{u}$ in cylindrical coordinates becomes

$$\nabla\mathbf{u}|_{\text{on particle}} = \begin{pmatrix} \frac{\partial\tilde{u}_r}{\partial r}\cos\varphi & \frac{\partial\tilde{u}_r}{\partial z}\cos\varphi & -\frac{\tilde{u}_r+\tilde{u}_\varphi}{r}\sin\varphi \\ \frac{\partial\tilde{u}_z}{\partial r}\cos\varphi & \frac{\partial\tilde{u}_z}{\partial z}\cos\varphi & -\frac{\tilde{u}_z}{r}\sin\varphi \\ \frac{\partial\tilde{u}_\varphi}{\partial r}\sin\varphi & \frac{\partial\tilde{u}_\varphi}{\partial z}\sin\varphi & \frac{\tilde{u}_\varphi+\tilde{u}_r}{r}\cos\varphi \end{pmatrix} \tag{28}$$

For a Newtonian fluid, the lift and drag forces can be calculated as

$$F_l^N = a^2 \int_0^{2\pi} \int_0^{\pi} (T_{\rho\rho}^N \cos\theta - T_{\rho\theta}^N \sin\theta) \sin\theta d\theta d\varphi = 0 \tag{29}$$

$$\begin{aligned} F_d^N &= a^2 \int_0^{2\pi} \int_0^{\pi} (T_{\rho\rho}^N \sin\theta\cos\varphi + T_{\rho\theta}^N \cos\theta\cos\varphi - T_{\rho\varphi}^N \sin\varphi) \sin\theta d\theta d\varphi \\ &= \pi a^2 \int_0^{\pi} (\tilde{T}_{\rho\rho}^N \sin\theta + \tilde{T}_{\rho\theta}^N \cos\theta - \tilde{T}_{\rho\varphi}^N) \sin\theta d\theta \end{aligned} \tag{30}$$

F_l^N is zero since $\int_0^{2\pi} \cos\varphi d\varphi = 0$. In calculating F_d^N, all terms are proportional to either $\int_0^{2\pi} \cos\varphi^2 d\varphi$ or $\int_0^{2\pi} \sin\varphi^2 d\varphi$ which gives rise to the π in front of the integral.

For the second-order fluid, after some simplifications, it can be shown that the lift and drag forces can be determined as

$$F_l = \pi a^2 \int_0^{\pi} (\tilde{T}_{\rho\rho} \cos\theta - \tilde{T}_{\rho\theta} \sin\theta) \sin\theta d\theta \neq 0 \tag{31}$$

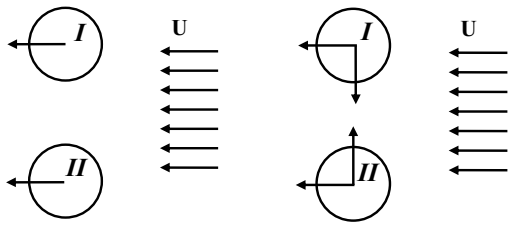

(a) Newtonian fluid (b) 2^{nd}-order fluid

FIG. 5: Schematic of the forces acting to two particles

$$F_d \;=\; F_d^N \tag{32}$$

The contribution of a second-order fluid to the lift force is proportional to either $\int_0^{2\pi} \cos\varphi^2 d\varphi$ or $\int_0^{2\pi} \sin\varphi^2 d\varphi$ thus a non-zero lift is applied to the particles. However, the contribution to the drag force is proportional to $\sin\varphi$ and $\cos\varphi$ or their cubes which all have zero integrals from 0 to π. Thus, the drag force in a second-order fluid is the same as for a Newtonian fluid. A schematic of the forces acting on the spheres in a Newtonian and a second-order fluid is shown in figure 5. If we define

$$\lambda_d = \frac{F_d}{6\pi\mu_f a U}, \quad \text{and} \qquad \lambda_l = \frac{F_l}{6\pi\mu_f a U} = \lambda_{De} De \tag{33}$$

the behavior of these coefficients versus particle separation are shown in figure 6. As it can be seen, the lift force decreases as the separation distance increases. One can show that the torque applied to these particles in a second-order fluid is the same as for a Newtonian fluid. $\lambda_t = \frac{Torque}{8\pi\mu_f U a^2}$ is plotted in figure 7. The shear and normal stresses on the surface of sphere I are shown in figure 8 for $\varphi = 0$ and in figure 9 for $\varphi = \frac{\pi}{2}$. The overall behavior is the same as in the case when the free stream is along the particles line of centers. The shear stress is the same in the second-order flow as in the Newtonian case. The normal stress and the pressure are not affected at the stagnation point $\theta = \frac{\pi}{2}$, whereas at other angles, a large compressive normal stress is observed ($\theta = 0$). For $\varphi = \frac{\pi}{2}$, the normal and shear stresses are zero in the Newtonian fluid but the pressure and normal stress are nonzero for the second-order fluid, as shown in figure 9.

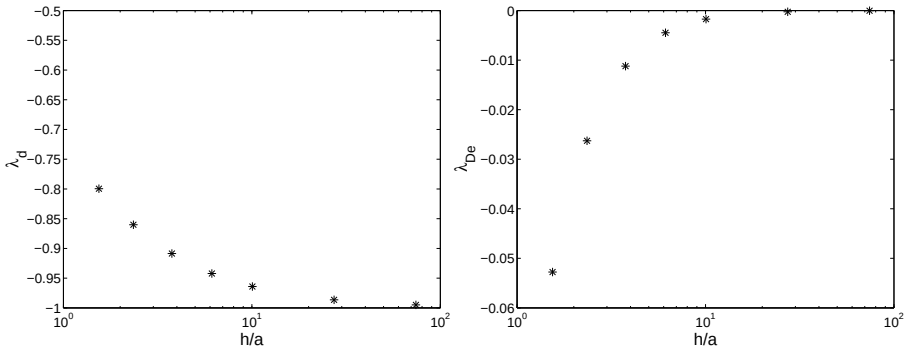

(a) (b)

FIG. 6: Force acting on the particle I in a second-order fluid while the free stream is perpendicular to the particles line of centers.

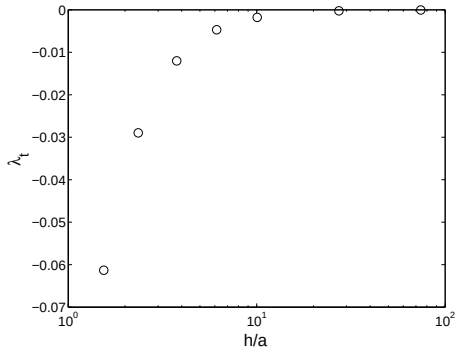

FIG. 7: Torque acting on sphere I in a second-order fluid while the free stream is perpendicular to the particles line of centers.

C. Two spherical particles in a free stream at an arbitrary angle

In this section, the more general case is studied when ζ (figure 1) is nonzero. Since the velocity field is obtained from the linear Stokes equations, superposition can be utilized to calculate the velocity field. However, the stress is nonlinear for a second-order fluid and the forces must be recalculated. $\nabla\mathbf{u}$ for the case when the free stream is perpendicular to the line of centers is given by equation (28) while for the case when the flow is along the line of centers, the velocity does not depend on φ and the last column and row in equation (9) are zero. One could now write $\mathbf{A}\nabla\mathbf{u}$, $\nabla\mathbf{u}^T\mathbf{A}$, and $\mathbf{A}^2$ where $\mathbf{u} = \mathbf{u}_\perp + \mathbf{u}\|$. Interestingly, the force due to the terms produced by products of $\perp$ and $\|$ are zero when one calculates the force along the line of centers. Thus, this force can be simply calculated by superposition of forces along the line of centers from the two previous sections. For the force perpendicular to the line of centers, the terms produced by products of $\perp$ and $\|$ are non-zero. Thus,

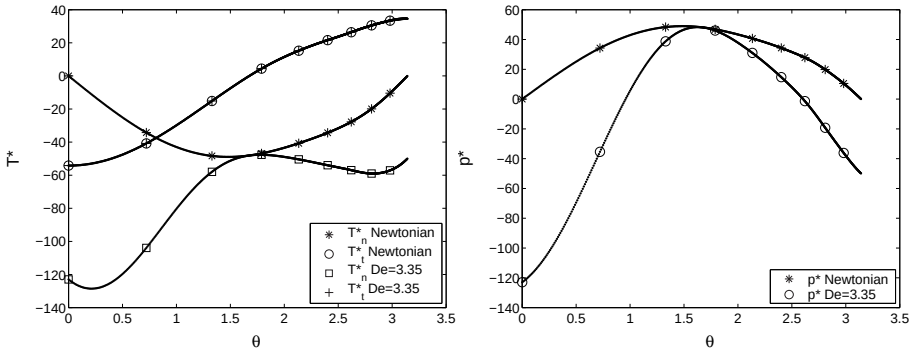

(a) Normal and shear stresses (b) Pressure

FIG. 8: Stresses on the surface of particle I in a second-order fluid when the flow is perpendicular to the line of centers. $Re = 0.05$, $De = 3.35$, $\frac{h}{a} = 1.543$, $\varphi = 0$.

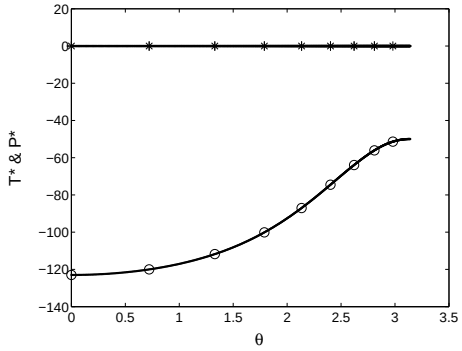

FIG. 9: Stresses on the surface of particle I in a second-order fluid when the flow is perpendicular to the line of centers. $(*)$ shear stress, (o) normal stress and pressure in second-order fluid. $Re = 0.05$, $De = 3.35$, $\frac{h}{a} = 1.543$, $\varphi = \frac{\pi}{2}$.

non-equal forces are applied to the particles perpendicularly to their line of centers. Figure 10 shows schematics of the forces acting on the particles. For this case

$$\lambda_{\perp} = \lambda_d + De\lambda_{De} = \frac{F_{\perp}}{6\pi\mu_f aU} \tag{34}$$

where $F_{\perp}$ is the force perpendicular to the line of centers. Figure 11(a) shows that the forces acting on the particles tend to rotate the line of centers until it becomes parallel to the free stream. This force decreases as the particles separate from each other and has a maximum when $\zeta = 45^o$ and is zero at $\zeta = 0^o$ or 90^o as shown in figure 11(b).

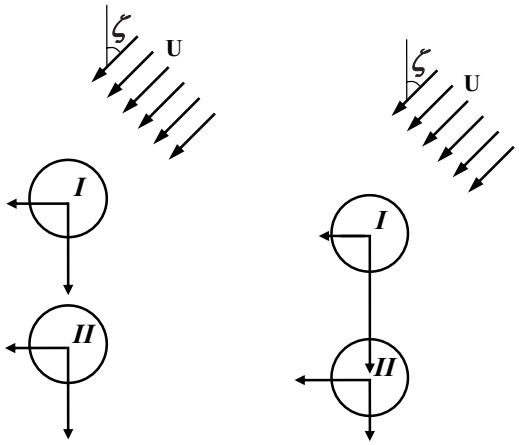

(a) Newtonian fluid (b) 2^{nd}-order fluid

FIG. 10: Schematic of the forces acting on two particles

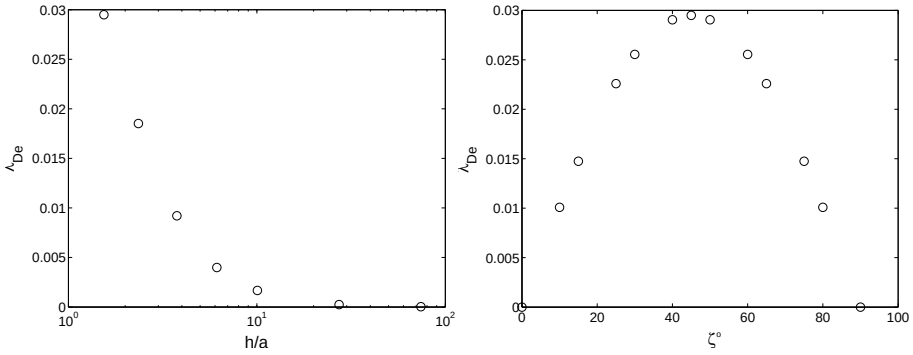

(a) (b)

FIG. 11: Forces acting on particle I in a second-order fluid in a free stream at an arbitrary angle. (a) λ_{De} versus particle separation distance when $\zeta = \frac{\pi}{4}$ (b)λ_{De} versus the free stream angle when $\frac{h}{a} = 1.543$

4. FORCES ACTING ON TWO FREELY-ROTATING FIXED SPHERES IN A FREE STREAM OF A SECOND-ORDER FLUID

As shown in figure 7, there is a torque experienced by non-rotating spheres in a free stream. Sedimenting spheres, unless experiencing an external torque (for example, generated by an electric field), cannot bear this torque and are hence prone to rotate such that they experience no torque. In order to analyze the forces applied to freely-rotating spheres in a free stream, one constructs a composite flow by adding the flow of two spheres counter-rotating in a quiescent fluid to the flow of two non-rotating spheres in a free stream examined previously.

At first, the forces acting on two rotating fixed spheres in a quiescent second-order fluid are considered. Sphere I is rotating with angular velocity $+\Omega$ and sphere II is rotating with angular velocity $-\Omega$ along y direction. The rotation rate Ω is chosen such that the torque experienced by each sphere in the composite flow is zero. In other words, the torque on the non-rotating sphere in the streaming flow is canceled by the torque acting on the same sphere rotating in a quiescent fluid. The pressure and velocity components can be described as follows

$$p_N^{r\dagger} = \mu_f \Omega W^{r\dagger} \cos\varphi \tag{35}$$

$$u_r^{r\dagger} = \frac{1}{2}\Omega[rW^{r\dagger} + c(X^{r\dagger} + Y^{r\dagger})]\cos\varphi = \tilde{u}_r^{r\dagger}\cos\varphi \tag{36}$$

$$u_\varphi^{r\dagger} = \frac{1}{2}\Omega c[(X^{r\dagger} - Y^{r\dagger})]\sin\varphi = \tilde{u}_\varphi^{r\dagger}\sin\varphi \tag{37}$$

$$u_z^{r\dagger} = \frac{1}{2}\Omega(zW^{r\dagger} + 2cZ^{r\dagger})\cos\varphi = \tilde{u}_z^{r\dagger}\cos\varphi \tag{38}$$

where the auxiliary functions $W^{r\dagger}$, $X^{r\dagger}$, $Y^{r\dagger}$, and $Z^{r\dagger}$ are defined in equations (24)-(27) replacing $\dagger$ with $r\dagger$ while the coefficients $A_n^{r\dagger}$ through $G_n^{r\dagger}$ are given by Goldman *et al.*[29] and Goldman[31]. The forces acting on the spheres can be calculated in a manner similar to that of Section 3 B and are shown in figure 12 where

$$\lambda_d = \frac{F_d}{6\pi\mu_f a^2\Omega}, \quad \text{and} \qquad \lambda_l = \frac{F_l}{6\pi\mu_f a^2\Omega} = \lambda_{De} De \tag{39}$$

It should be noted that the substantial time derivative of the Newtonian pressure plays a role here since the velocity of the surface of the spheres is not zero. The torque applied to the spheres rotating in a quiescent second-order fluid is the same as that for a Newtonian fluid. $\lambda_t = \frac{Torque}{8\pi\mu_f\Omega a^3}$ is plotted in figure 13. As mentioned above, the rotation rate Ω can be calculated such that the torque experienced by each sphere in the composite flow is zero. The rotation rate Ω for freely rotating spheres in a free stream of second-order fluid is plotted in figure 14.

In order to compute the attractive forces between the freely rotating spheres, the velocity field for two non-rotating spheres in a free stream and two rotating spheres in a quiescent flow will be superimposed and the stresses for this new field will be calculated. The shear-rate distribution on a sphere for both the freely-rotating and non-rotating cases is shown in

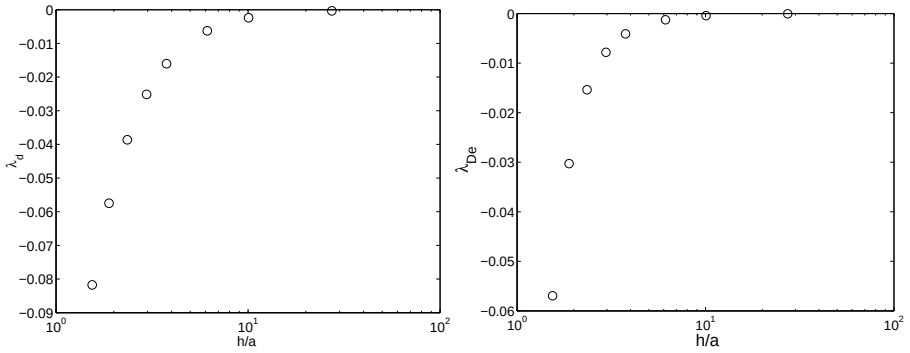

(a) (b)

FIG. 12: Force acting on the particle I while the spheres are rotating in a quiescent second-order fluid.

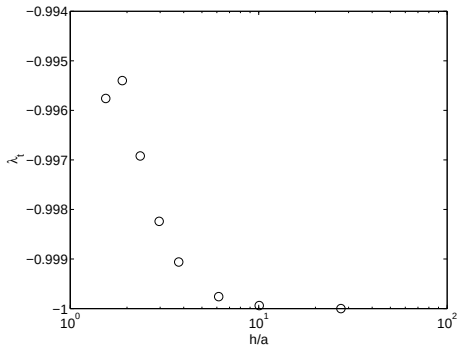

FIG. 13: Torque acting on sphere I while the spheres are rotating in a quiescent second-order fluid.

figure 15a). The shear-rate is smaller on the outermost edges ($\theta = 0$ for sphere I) of freely rotating spheres and larger on the innermost edges. The viscoelastic pressure is proportional to the square of the local shear rate As it can be seen, the modification of the pressure due

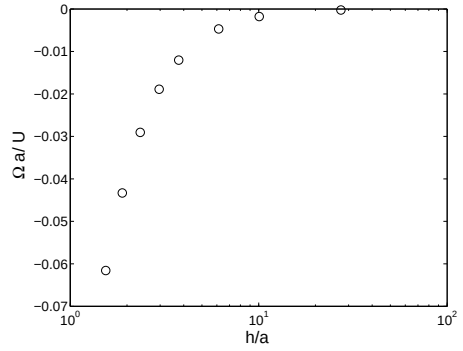

FIG. 14: Rotation rate of freely-rotating spheres in a free stream of a second-order fluid.

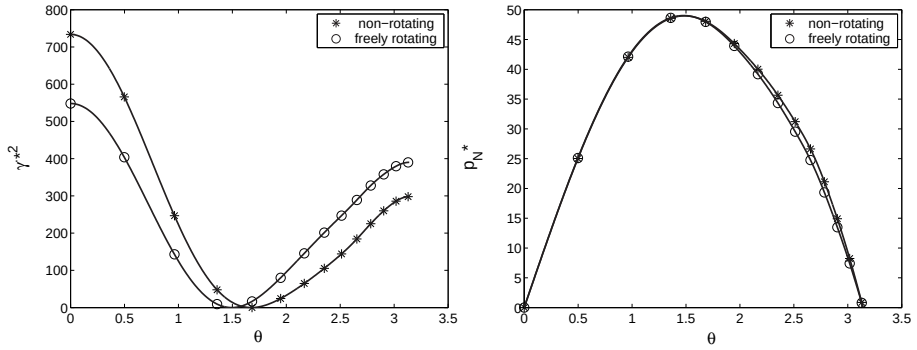

(a) (b)

FIG. 15: The distribution of shear rate ($\dot{\gamma}^{*2} = \frac{1}{2} tr\mathbf{A}^{*2}$)) and Stokes pressure on the surface of sphere I for non-rotating and freely rotating spheres. $Re = 0.05$, $De = 3.35$, $\frac{h}{a} = 1.543$, $\varphi = 0$.

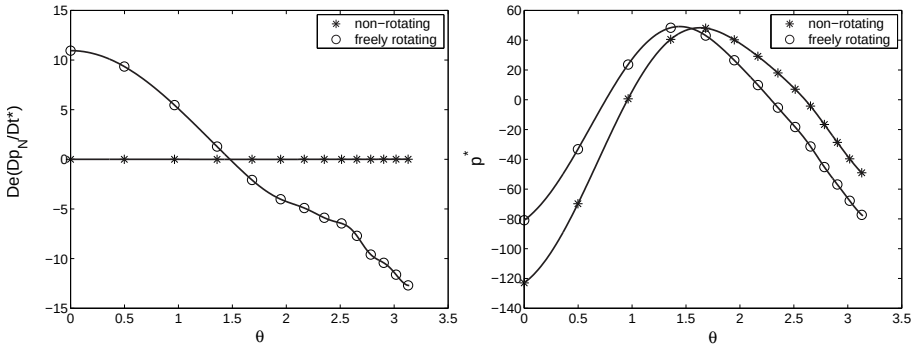

(a) (b)

FIG. 16: The distribution of $De\frac{Dp^*}{Dt^*}$ and pressure on the surface of sphere I for non-rotating and freely rotating spheres. $Re = 0.05$, $De = 3.35$, $\frac{h}{a} = 1.543$, $\varphi = 0$.

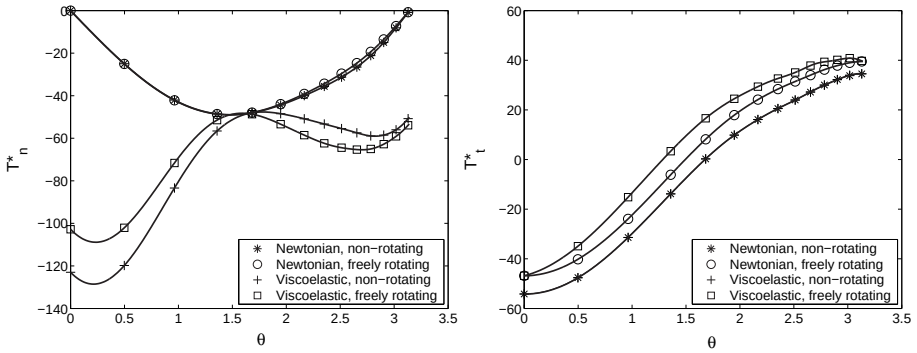

(a) (b)

FIG. 17: The distribution of normal and shear stresses on the surface of sphere I for non-rotating and freely rotating spheres. $Re = 0.05$, $De = 3.35$, $\frac{h}{a} = 1.543$, $\varphi = 0$.

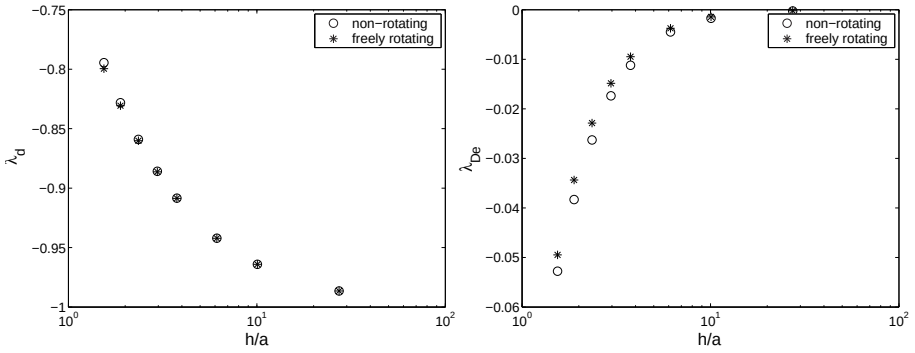

(a) (b)

FIG. 18: Forces acting on the particle sphere I for non-rotating and freely rotating spheres.

to shear rate enhances the attraction between the spheres for the freely-rotating case. P_N^*, $De\frac{Dp^*}{Dt^*}$, and p^* are shown in figure 15b), 16a), and b). In fact, all three terms in equation 5, the Stokes pressure, time derivative of Stokes pressure, and viscoelastic pressure, change the pressure in the same way and enhance the attraction force. However, the total lift force on the particles is less than the one for non-rotating particles due to the modification of the first and second Rivlin-Ericson tensors. The normal and shear stresses are plotted in figure 17. The drag and lift forces on the particles are shown in figure 18. As it can be seen, a larger drag and smaller lift forces act on freely rotating spheres as compared to non-rotating ones.

It can be concluded that rotation of the spheres mitigates the attraction. The substantial time derivative of the pressure is taken into account since the velocity is non-zero on the surface of the spheres. The effect of rotation is only a small percentage of the effect of translation on the particles' attraction as shown in figure 18.

5. VISCOUS POTENTIAL FLOW

The shear stress and tangential velocity on the boundary are in general discontinuous in viscous and viscoelastic irrotational flows. However, in some cases such as flow near the stagnation points, the amount of shear is small[32]. In this section, normal stresses on the surface of two spheres in a uniform free stream along their line of centers are analyzed utilizing viscoelastic potential flow. A similar calculation is performed by ardekani et al.[14] for a particle moving normal to a wall. A summary of the calculations is given here for

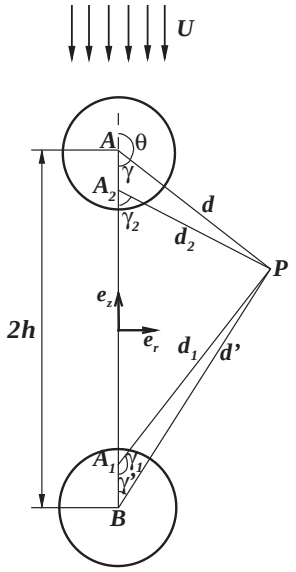

FIG. 19: Two spherical particles in a free stream

completeness.

It has been shown that for potential flow where $\mathbf{u} = \nabla\phi$[33]

$$\nabla \cdot (\alpha_1 \mathbf{B} + \alpha_2 \mathbf{A}^2) = (3\alpha_1 + 2\alpha_2)\nabla\chi \tag{40}$$

where

$$\chi = \frac{\partial^2\phi}{\partial x_i \partial x_j}\frac{\partial^2\phi}{\partial x_i \partial x_j} = \frac{1}{4} tr\mathbf{A}^2 \tag{41}$$

Thus, the divergence of the stress is irrotational. Using equations (40) and (41), Wang and Joseph[34] noted that the pressure can be calculated using the Bernoulli equation as

$$\rho\frac{\partial\phi}{\partial t} + \frac{1}{2}\rho|\nabla\phi|^2 + p - \beta\chi = C(t) \tag{42}$$

Using equations (3) and (42), the stress tensor for viscoelastic potential flow becomes

$$\mathbf{T} = \left[\rho\frac{\partial\phi}{\partial t} + \frac{1}{2}\rho|\nabla\phi|^2 - \beta\chi - C(t)\right]\mathbf{I} + \left[\mu + \alpha_1\left(\frac{\partial}{\partial t} + \mathbf{u}\cdot\nabla\right)\right]\mathbf{A} + (\alpha_1 + \alpha_2)\mathbf{A}^2 \tag{43}$$

For two spherical particles in a free stream as shown in Figure 19, the potential-flow solution can be obtained using the image of a doublet source in a sphere and is given as the

following series[35]

$$\begin{aligned}\phi = -Uz \;+\; U(&\frac{\mu_0 \cos\gamma}{d^2} + \frac{\mu_1 \cos\gamma_1}{d_1^2} + \frac{\mu_2 \cos\gamma_2}{d_2^2} + ...) \\ -\; U(&\frac{\mu_0 \cos\gamma'}{d'^2} + \frac{\mu_1 \cos\gamma_1'}{d_1'^2} + \frac{\mu_2 \cos\gamma_2'}{d_2'^2} + ...)\end{aligned} \tag{44}$$

where $\mu_0 = \frac{1}{2}a^3$, U is the particle velocity, A is the center of sphere I, and B is the center of sphere II, $d = AP$, $d' = BP$, $d_1 = A_1P$, $d_1' = B_1P$, etc., are the distances between the doublets and a fixed point P which can be defined using

$$\begin{aligned}
f_1 &= c' - \frac{a^2}{c'}, \qquad f_2 = \frac{a^2}{f_1}, \quad \frac{\mu_1}{\mu_0} = -\frac{a^3}{c'^3}, \qquad \frac{\mu_2}{\mu_1} = -\frac{a^3}{f_1^3} \\
f_3 &= c' - \frac{a^2}{c' - f_2}, \quad f_4 = \frac{a^2}{f_3}, \quad \frac{\mu_3}{\mu_2} = -\frac{a^3}{(c' - f_2)^3}, \quad \frac{\mu_4}{\mu_3} = -\frac{a^3}{f_3^3} \\
f_5 &= c' - \frac{a^2}{c' - f_4}, \quad f_6 = \frac{a^2}{f_5}, \quad \frac{\mu_5}{\mu_4} = -\frac{a^3}{(c' - f_4)^3}, \quad \frac{\mu_6}{\mu_5} = -\frac{a^3}{f_5^3}, ...
\end{aligned} \tag{45}$$

where $c' = 2h$ is twice of the separation distance between the two spheres; $AA_1 = f_1$, $AA_2 = f_2$, etc. (γ, d, and other parameters are shown in figure 19 for clarification.)

$$\mathbf{A} = U\tilde{\mathbf{A}} = 2U \begin{pmatrix} \frac{\partial^2\varphi}{\partial r^2} & \frac{\partial^2\varphi}{\partial r \partial z} & 0 \\ \frac{\partial^2\varphi}{\partial r \partial z} & \frac{\partial^2\varphi}{\partial z^2} & 0 \\ 0 & 0 & \frac{1}{r}\frac{\partial\varphi}{\partial r} \end{pmatrix} \tag{46}$$

where r and z are cylindrical coordinates as shown in figure 19. The stress tensor can be written as

$$\begin{aligned}
\mathbf{T} + C\mathbf{I} \;=\; &\mu\tilde{\mathbf{A}}U + \Bigg(\Bigg[\frac{1}{2}\rho \left\{ (\frac{\partial\varphi}{\partial r})^2 + (\frac{\partial\varphi}{\partial z})^2 \right\} \\
&-\; \beta \left\{ (\frac{\partial^2\varphi}{\partial r^2})^2 + (\frac{1}{r}\frac{\partial\varphi}{\partial r})^2 + (\frac{\partial^2\varphi}{\partial z^2})^2 + 2(\frac{\partial^2\varphi}{\partial r \partial z})^2 \right\} \Bigg] \mathbf{I} \\
&+\; \alpha_1 \tilde{\mathbf{u}} \cdot \nabla\tilde{\mathbf{A}} + (\alpha_1 + \alpha_2)\tilde{\mathbf{A}}^2 \Bigg) U^2
\end{aligned} \tag{47}$$

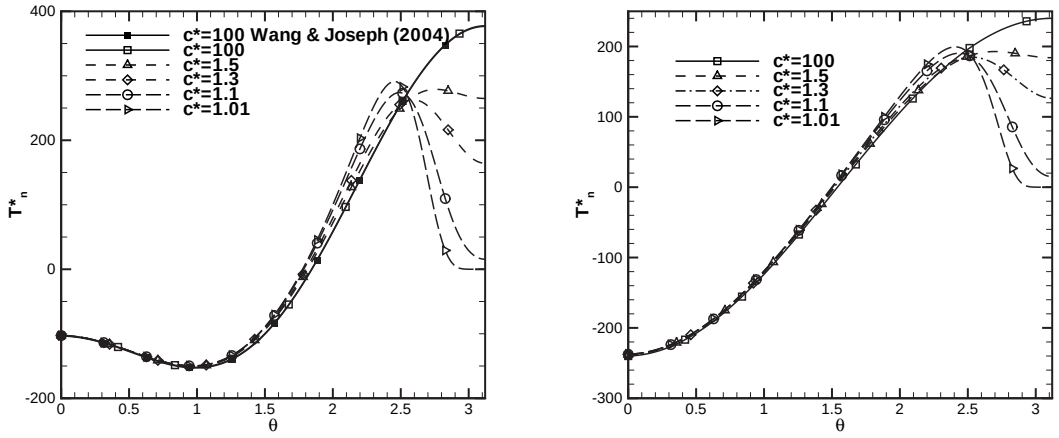

(a) Second-order fluid (b) Newtonian fluid

FIG. 20: Two spherical particles in a free stream at $Re = 0.05$, $a = 1cm$, $De = 0.168$, $c^* = \frac{c}{2a}$. Normal stress at surface of sphere I is shown.

while the normal stress T_n and the shear stress T_t are

$$\begin{aligned} T_n &= T_{rr}\sin^2\theta + T_{zz}\cos^2\theta + T_{rz}\sin 2\theta \\ T_t &= \frac{T_{rr} - T_{zz}}{2}\sin 2\theta + T_{rz}\cos 2\theta \end{aligned} \tag{48}$$

Using equations (44), (47), and (48), the normal stress is computed on the surface of sphere I in a free stream. Properties of liquid M1 with density $\rho = 0.895\ gcm^{-3}$, $\alpha_1 = -3$, and $\alpha_2 = 5.34\ gcm^{-1}$[36] are utilized. Figure 20 shows the dimensionless normal stress on the surface of sphere I as a function of θ for different separation distances between the two particles. All terms of equation (43) are included in figures 20, 21, and 22. Results for $Re = 0.05$ and $De = 0.168$ are shown which agree with the published results by Wang and Joseph[34] when $c \to \infty$. It can be seen that for large separation distances, a tensile normal stress occurs at the trailing edge when the fluid is Newtonian, and that for a second-order fluid, this tensile stress is even larger. When the particle separation decreases in either a Newtonian or a second-order fluid, the tensile stress at the trailing edge of sphere I decreases whereas the normal stress at the leading edge does not change. In figure 21, the normal stress acting on the surface of sphere II is shown. The normal stress at the stagnation point predicted by viscoelastic potential flow (VPF) is noticeably different in the Newtonian and the second-order fluid, a result which disagrees with the results obtained employing

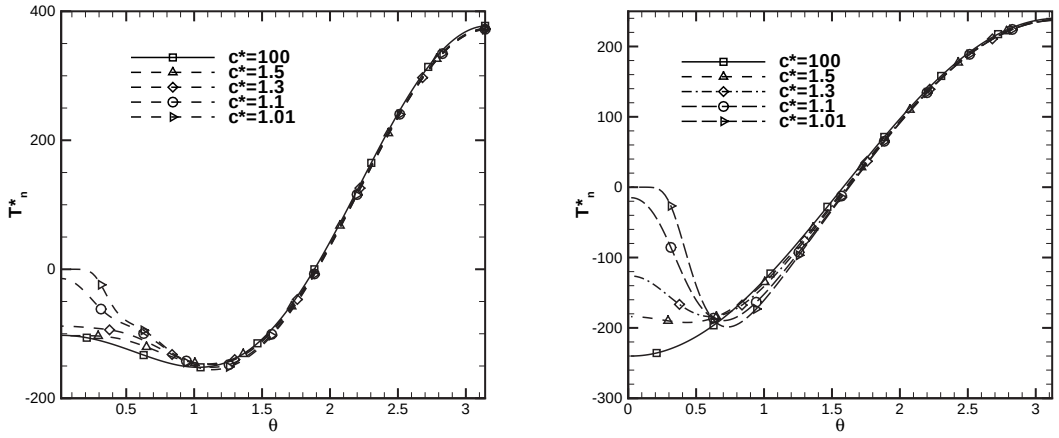

(a) Second-order fluid (b) Newtonian fluid

FIG. 21: Two spherical particles in a free stream at $Re = 0.05$, $a = 1cm$, $De = 0.168$, $c^* = \frac{c}{2a}$. Normal stress at surface of sphere II is shown.

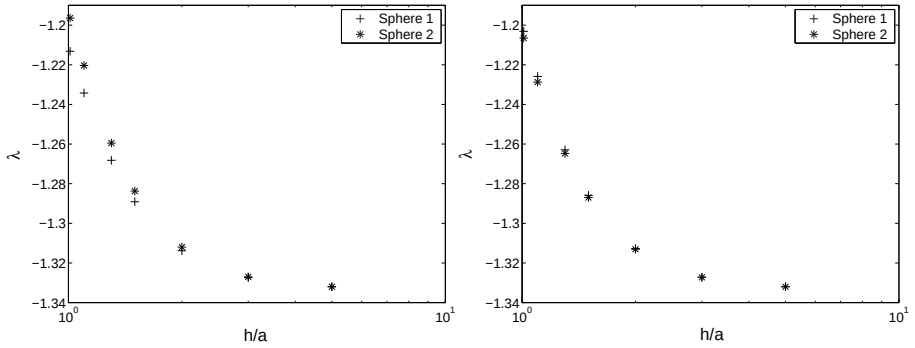

(a) Second-order fluid (b) Newtonian fluid

FIG. 22: Two spherical particles in a free stream at $Re = 0.05$, $De = 0.168$.

the Stokes equations. The normal stress is integrated over the sphere surface and the forces applied to the particles are calculated and shown in figures 22(a) and 22(b). These forces are not necessary quantitatively correct since our argument for the use of VPF is only valid near the stagnation points. A smaller drag force acts on the leading sphere in the Newtonian fluid, whereas a larger drag force acts on the leading sphere in the second-order fluid. A repulsive force is predicted using VPF in the Newtonian case while an attractive force is obtained in the second-order fluid. The repulsive force acting on the particles in a Newtonian fluid is due to inertia. These results show that if one adds the effect of inertia to the results of the previous sections, critical separation in the second-order fluid might be predicted. Finally,

our explanations of the aggregation of particles in viscoelastic fluids rest on three pillars; the first is a viscoelastic "pressure" generated by normal stresses due to shear. Secondly, the total time derivative of the pressure is an important factor in the forces applied to moving particles. The third is associated with a change in the normal stress at points of stagnation which is a purely extensional effect unrelated to shearing.

6. CONCLUSIONS

The forces acting on two non-rotating spherical particles in a second-order fluid in Stokes flow are calculated. The results are in agreement with experimental observations. The contribution of the second-order fluid to the forces acting on the particles is an attractive force when the free stream is along or perpendicular to the line of centers. For flow at an angle, these forces act in the direction that rotates the line of centers until it becomes parallel to the free stream.

The results for freely rotating spheres show that rotation of the spheres mitigates the attraction. The substantial time derivative of the pressure is taken into account since the velocity is non-zero on the surface of the spheres and it enhances the attraction. However, the effect of rotation is only a small percentage of the effect of translation on the particles' attraction.

7. ACKNOWLEDGMENT

This work is sponsored by National Science Foundation under grants CBET-0302837 and OISE-0530270. The first author acknowledges the Zonta International Foundation for an Amelia Earhart fellowship.

---

[1] J. Happel and H. Brenner, *Low Reynolds Number Hydrodynamics* (Prentice-Hall, Englewood Cliffs, NJ, 1965), chap. 6, pp. 235–244.

[2] H. L. Goldsmith and S. G. Mason, *The microrheology of dispersions* (Academic, New York, 1967), vol. 4, pp. 85–260.

[3] B. Caswell, "Sedimetation of particles in non-newtonian fluids", ASME **22** (1977).

[4] L. G. Leal, "The motion of small particles in non-Newtonian fluids", J. Fluid Mech. **5**, 33 (1979).

[5] A. M. Ardekani and R. H. Rangel, "Unsteady motion of two solid spheres in Stokes flow", Phys. of Fluids **18** (2006).

[6] A. M. Ardekani and R. H. Rangel, "Numerical investigation of particle-particle and particle-wall collisions in a viscous fluid", J. Fluid Mech. **accepted** (2007).

[7] D. D. Joseph, T. Funada, and J. Wang, *Potential Flows of Viscous and Viscoelastic Fluids* (Cambridge University Press, Cambridge, 2007).

[8] B. Coleman and W. Noll, "An approximation theorem for functionals, with applications in continum mechanics", Arch. Ration. Mech. Anal. **6**, 355 (1960).

[9] R. S. Rivlin and J. L. Ericksen, "Stress deformation relations for isotropic materials", J. Rat. Mech. Anal **4**, 323 (1955).

[10] R. Bird, R. Armstrong, and Hassager, *Dynamics of polymeric Liquids* (John Wiley, New York, 1987).

[11] D. D. Joseph, *Dynamics of viscoelastic Liquids* (Springer, New York, 1990).

[12] L. G. Leal, "The slow motion of slender rod-like particles in a second-order fluid", J. Fluid Mech. **69**, 305 (1975).

[13] B. P. Ho and L. G. Leal, "Migration of rigid spheres in a two-dimensional unidirectional shear flow of a second-order fluid", J. Fluid Mech. **79**, 783 (1976).

[14] A. M. Ardekani, R. H. Rangel, and D. D. Joseph, "Motion of a sphere normal to a wall in a second-order fluid", J. Fluid Mech. **587**, 163 (2007).

[15] M. J. Riddle, C. Narvaez, and R. Bird, "Interactions between two spheres falling along their line of centers in viscoelastic fluid", J. Non-Newtonian Fluid Mech. **2**, 23 (1977).

[16] P. Brunn, "Interaction of spheres in a viscoelastic fluid", Rheologica Acta **16**, 461 (1977).

[17] P. Brunn, "Slow motion of a rigid particle in a 2nd-order fluid", J. Fluid Mech. **82**, 529 (1977).

[18] R. J. Phillips, "Dynamic simulation of hydrodynamically interacting spheres in a quiescent second-order fluid", J. Fluid Mech. **315**, 345 (1996).

[19] H. Binous and R. J. Phillips, "Dynamic simulation of one and two particles sedimenting in viscoelastic suspensions of FENE dumbbells", J. Non-Newtonian Fluid Mech. **83**, 93 (1999).

[20] E. T. G. Bot, M. A. Hulsen, and B. H. A. A. van den Brule, "The motion of two spheres falling along their line of centres in a Boger fluid", J. Non-Newtonian Fluid Mech. **79**, 191 (1998).

[21] D. D. Joseph and J. Feng, "A note on the forces that move particles in a second-order fluid",

J. Non-Newtonian Fluid Mech. **64**, 299 (1996).

[22] R. J. Phillips and L. Talini, "Chaining of weakly interacting particles suspended in viscoelastic fluids", J. Non-Newtonian Fluid Mech. **147**, 175 (2007).

[23] S. Takagi, H. Oguz, Z. Zhang, and A. Prosperetti, "A new method for particle simulation part ii: Two-dimensional Navier-Stokes flow around cylinders", J. Comput. Phys. **187**, 371 (2003).

[24] O. G. Harlen, J. M. Rallison, and M. D. Chilcott, "High-Deborah-number flows of dilute polymer solutions", J. Non-Newtonian Fluid Mech. **34**, 319 (1990).

[25] R. Tanner, "Plane creeping flows of in compressible second-order fluids", Phys. Fluids **9**, 1246 (1966).

[26] M. Stimson and G. B. Jeffery, "The motion of two spheres in a viscous fluid", Proc. R. Soc. London, Ser. A **111**, 110 (1926).

[27] L. Pasol, M. Chaoui, S. Yahiaoui, and F. Feuillebois, "Analytic solution for a spherical particle near a wall in axisymmetrical polynimial creeping flows", Phys. Fluids **17** (2005).

[28] G. B. Jeffery, "On a form of the solution of Laplace's equation suitable for problems relating to two spheres", Proc. R. Soc. London, Ser. A **87**, 109 (1912).

[29] A. J. Goldman, R. G. Cox, and H. Brenner, "The slow motion of two identical arbitrary oriented spheres through a viscous fluid", Chemical Eng. Science **21**, 1151 (1966).

[30] M. E. O'Neill, "Exact solutions of the equations of slow viscous flow gerated by the asymmetrical motion of two equal spheres", Appl. Sci. Res. **21**, 452 (1970).

[31] A. J. Goldman, "investigation in low Reynolds number fluid-particle dynamics", Ph.D. thesis, New York University (1966).

[32] D. D. Joseph and J. Wang, "The dissipation approximation and viscous potential", J. Fluid Mech. **505**, 365 (2004).

[33] D. D. Joseph, "Bernoulli equation and the competition of elastic and inertial pressure in the potential flow of a second-order fluid", J. Non-Newtonian Fluid Mech. **42**, 358 (1992).

[34] J. Wang and D. D. Joseph, "Potential flow of a second-order fluid over a sphere or an eclipse", J. Fluid Mech. **511**, 201 (2004).

[35] H. Lamb, *Hydrodynamics* (Dover, New York, 1945).

[36] H. H. Hu, O. Riccius, K. P. Chen, M. Arney, and D. D. Joseph, "Climbing constant, second-order correction of Trouton's viscosity, wave speed and delayed die swell for M1", J. Non-Newtonian Fluid Mech. **35**, 287 (1990).